Natural Resources Canada
Ressources naturelles Canada

CANADIAN GEOSCIENCE MAP 159

GEOLOGY

BAIE VERTE AND PARTS OF FLEUR DE LYS

Newfoundland and Labrador
NTS 12-H/16 and part of NTS 12-I/1

Map Information Document

Canadian Geoscience Maps

2015

Canada

PUBLICATION

Map Number

Natural Resources Canada, Geological Survey of Canada
Canadian Geoscience Map 159

Title

Geology, Baie Verte and parts of Fleur De Lys, Newfoundland and Labrador, NTS 12-H/16 and part of NTS 12-I/1

Scale

1:50 000

Catalogue Information

Catalogue No. M183-1/159-2013E-PDF
ISBN 978-1-100-22549-4
doi:10.4095/295865

Recommended Citation

Skulski, T., Castonguay, S., Kidd, W.S.F., McNicoll, V.J., van Staal, C.R., and Hibbard, J.P., 2015. Geology, Baie Verte and parts of Fleur de Lys, Newfoundland and Labrador, NTS 12-H/16 and part of NTS 12-I/1; Geological Survey of Canada, Canadian Geoscience Map 159, scale 1:50 000. doi:10.4095/295865

ABSTRACT

Northwestern Baie Verte Peninsula (Newfoundland and Labrador, NTS 12-H/16 and part of 12-I/2) is underlain by Mesoproterozoic basement of the East Pond Metamorphic Suite; Neoproterozoic to Ordovician Laurentian continental margin rocks of the Fleur de Lys Supergroup; Cambrian dismembered ophiolite including Pacquet, Point Rousse, and Advocate complexes; submarine Ordovician ophiolite cover of the Snooks Arm Group; and Ordovician-Silurian, continental plutonic rocks of the Burlington plutonic suite and overlying Silurian Micmac Lake Group; King's Point volcanic complex; and Cape St. John Group and related plutons. Ten mines have operated in this area (two current, eight past-producing). The ophiolitic rocks host Cu-Au volcanogenic massive-sulphide (Terra Nova, Rambler Main, Big Rambler Pond, East, Ming, and Ming West mines) and asbestos deposits (Advocate mine). The Snooks Arm Group hosts three gold deposits (Goldenville, Stog'er Tight, and Pine Cove mines). Four phases of regional deformation affected this area including D_1, best documented in the Birchy Complex, is related to ophiolite obduction; D_2, regional, penetrative deformation was accompanied by greenschist- to amphibolite-facies metamorphism; D_3, related to folds, commonly asymmetric; and D_4, related to recumbent folding in the northeast and extensional and dextral faults and reactivation of faults.

RÉSUMÉ

Le sous-sol de la partie nord-ouest de la péninsule Baie Verte (Terre-Neuve-et-Labrador, SNRC 12-H/16 et une partie de 12-I/2) est constitué d'un socle mésoprotérozoïque formé de la Suite métamorphique d'East Pond; de roches du Néoprotérozoïque à l'Ordovicien de la marge laurentienne appartenant au Supergroupe de Fleur de Lys; d'ophiolites démembrées du Cambrien des complexes de Pacquet, de Point Rousse et d'Advocate; de la succession sous-marine de couverture des ophiolites de l'Ordovicien du Groupe de Snooks Arm; des roches plutoniques continentales de la suite plutonique de Burlington de l'Ordovicien-Silurien; ainsi que des unités sus-jacentes du Silurien constituées du Groupe de Micmac Lake, du complexe volcanique de King's Point et du Groupe de Cape St. John et des plutons apparentés. Dix mines ont été exploitées dans cette région (deux actives, huit anciennes). Les ophiolites sont les hôtes de gisements de sulfures massifs volcanogènes riches en cuivre-or (mines Terra Nova, Rambler Main, Big Rambler Pond, East, Ming et Ming West) et d'amiante (mine Advocate). Le Groupe de Snooks Arm est l'hôte de trois gisements d'or (mines Goldenville, Stog'er Tight et Pine Cove). Quatre phases de déformation régionales ont touché la région, dont : D_1, documentée le mieux dans le Complexe de Birchy, est reliée à l'obduction des ophiolites; D_2, une déformation régionale et pénétrative, a été accompagnée d'un métamorphisme du faciès des schistes verts au faciès des amphibolites; D_3, rapportée à des plis, communément asymétriques; et D_4, rapportée à la formation de plis couchés dans le nord-est et à la formation de failles d'extension et de failles dextres ainsi qu'à la réactivation de failles.

ABOUT THE MAP

General Information

Authors: T. Skulski, S. Castonguay, W.S.F. Kidd, V.J. McNicoll, C.R. van Staal, and J.P. Hibbard

Geology by T. Skulski, S. Castonguay, and C.R. van Staal; I. Kerr (University of Victoria); Y. Moussallam (University of Ottawa); S. Hinchey (Memorial University); 2006–2008; W.S.F. Kidd (Cambridge University), 1970–1971; and J. Hibbard (Geological Survey of Newfoundland and Labrador), 1976–1982

Geological compilation by T. Skulski and S. Castonguay, 2008–2013

Geophysical and remotely sensed data processed by H. Slavinski, B. Spicer, W. Morris, H. Ugalde (McMaster University), 2007; G. Kilfoil (Geological Survey of Newfoundland and Labrador), 2007; and T. Skulski, 2008–2013

Compiled structural data digitized by M. Currie, B.Harris, and A. Magee

Cartography by N. Côté

Critical review by A. Zagorevski (Geological Survey of Canada) and H.A. Sandeman (Geological Survey of Newfoundland and Labrador)

Scientific editing by E. Inglis

Initiative of the Geological Survey of Canada, conducted under the auspices of the Appalachian TGI-3 Project as part of Natural Resources Canada's Targeted Geoscience Initiative (TGI-3).

Map projection Universal Transverse Mercator, zone 21.
North American Datum 1983

Base map at the scale of 1:50 000 from Natural Resources Canada, with modifications.
Elevations in metres above mean sea level

Magnetic declination 2015, 19°56'W, decreasing 11.6' annually.

This map is not to be used for navigational purposes.

Title photograph: Sheeted dykes of the Point Rousse Complex, west shore Ming's Bight, Newfoundland and Labrador. Photograph by S. Castonguay. 2014-110

The Geological Survey of Canada welcomes corrections or additional information from users.

Data may include additional observations not portrayed on this map.
See documentation accompanying the data.

This publication is available for free download through GEOSCAN (http://geoscan.nrcan.gc.ca/).

Map Viewing Files
The published map is distributed as a Portable Document File (PDF), and may contain a subset of the overall geological data for legibility reasons at the publication scale.

ABOUT THE GEOLOGY

Descriptive Notes

The Baie Verte map area in the northwest part of Baie Verte Peninsula (Newfoundland and Labrador) is one of three 1:50 000 scale maps in this area that are based on new and compiled bedrock geological and remotely sensed data (Fig. 1; Skulski et al., 2015a, b). This part of the Newfoundland Appalachians is underlain by Mesoproterozoic basement rocks, Neoproterozoic to Ordovician rocks of the Humber continental margin, dismembered Cambrian ophiolite, Ordovician ophiolite cover, and Upper Ordovician to Silurian continental volcano-plutonic complexes (Fig. 2; IUGS Time Scale of Cohen et al. (2013) is utilized herein).

TECTONOSTRATIGRAPHY AND SETTING

The East Pond Metamorphic Suite constitutes Mesoproterozoic basement (de Wit, 1980, de Wit and Armstrong, 2014) to the overlying Fleur de Lys Supergroup and consists of psammitic and semipelitic gneiss, quartzite, amphibolite, migmatitic gneiss, and granitic gneiss (unit mPEPm). The overlying Fleur de Lys Supergroup represents the Humber continental margin that now comprises three tectonic entities (van Staal et al., 2013): the ocean-continent transition (Birchy Complex), an extensional allochthon (Rattling Brook Group), and a para-autochthonous continental margin (Ming's Bight, Old House Cove, and White Bay groups). The Birchy Complex includes: interbedded psammite and pelite (unit nPBq) overlain by tholeiitic metabasalt and mafic metatuff cut by metagabbro sills and dykes (unit nPBm), coarse-grained mafic metaclastic rocks (unit nPBe), and coarse-grained gabbro sills dated at 558.3 ± 0.7 Ma (location 25, Table 1; unit nPBg). These are overlain by interbedded psammite, semipelite with coticules, minor metabasalt and gabbro, intermediate tuff dated at 556 ± 4 Ma (location 24, Table 1), and tectonic mélange including large chaotic blocks of serpentinized ultramafic rock (unit nPOu), metapyroxenite, metagabbro, mafic volcanic and metasedimentary clasts, and locally, ultramafic-mafic–derived wacke (unit nPBc). These are intruded by quartz diorite and trondhjemite (unit nPBt) and overlain by graphitic pelite (unit nPBp) and calcareous semipelite (unit nPBcp). The Flat Point Formation (unit nPBFP) lies at the top of the Birchy Complex, resembles units in the Rattling Brook Group and consists of psammitic schist, metawacke, and pebbly conglomerate. Detrital zircon grains in Flat Point psammite have a Laurentian provenance and maximum depositional age of 990 ± 52 Ma (van Staal et al., 2013). The Rattling Brook Group, believed to originally conformably overlie the Birchy Complex (van Staal et al., 2013), comprises massive to possibly pillowed, conformable mafic schist and amphibolite (unit nPORBa) overlain by graphitic schist (locally unit nPORBg), marble, calcareous pelite, and marble breccia (unit nPORBm). Para-autochthonous Humber margin rocks include Ediacaran rift-facies and Cambrian to Early Ordovician drift-facies metasedimentary rocks (carbonate and transgressive clastic sediments) subdivided into three, likely coeval, tectonostratigraphic groups that basinward include the White Bay (west of present map area), Old House Cove, and Ming's Bight groups. The Ming's Bight Group is exposed east of Ming's Bight in a Devonian extensional uplift (Anderson et al., 2001). It includes psammite, semipelitic schist, quartz-pebble conglomerate, and graphitic schist with pods of metagabbro and metapyroxenite (unit nPOMB). The metaclastic rocks are associated with panels of massive to pillowed, tholeiitic metabasalt and amphibolite (Pelly Point schist of Hibbard (1983)), that are correlated with the Birchy Complex. The Old House Cove Group includes a lower polymict metaconglomerate (Middle Arm Metaconglomerate; unit nPOOHc) that unconformably overlies the East Pond Metamorphic Suite (de Wit, 1980; unit mPEPm). The basement and metaconglomerate are separated from the Old House Cove Group by tectonized mica schist (unit nPOHt). Structurally overlying psammite, semipelitic schist, minor pebbly psammitic schist, graphitic schist (unit nPOOHp), massive amphibolite (unit nPOOHa), and marble and calcareous pelite (unit nPOOHm) make up the rest of the group. Amphibolitized eclogitic gabbro sills and dykes (unit nPOae) locally cut the East Pond Metamorphic Suite and Middle Arm Metaconglomerate. Massive amphibolite dykes, sills, and pods (unit nPOa) cut the Old House Cove Group. Serpentinized ultramafic rocks (unit nPOu) occur as meter- to decimetre-scale lenses or

as fault-bounded slivers and may represent mantle (metaharzburgite; van Staal et al. (2013)) and or ultramafic cumulate rocks.

The Baie Verte Line (Hibbard, 1983) is a steeply dipping, reworked tectonic zone that separates the Humber margin to the west, from the Baie Verte Oceanic Tract and its ophiolite cover to the east. The Baie Verte Oceanic Tract includes intact ophiolite of the Betts Cove Complex to the east and correlative, but dismembered ophiolite complexes that expose progressively deeper structural levels toward the west. The Pacquet complex only exposes the volcanic section comprising pillowed boninite of the Betts Head Formation (unit ЄBHb), locally interbedded with thin felsic volcanic flows (unit ЄBHf), overlain by plagioclase-phyric, island-arc tholeiitic basalt and boninite units of the Mount Misery Formation (unit ЄMMm). These are capped by a felsic volcanic dome comprising fragmental rocks (unit ЄRRt) and flows (unit ЄRRl) of the Rambler Rhyolite formation dated at 487 ± 4 Ma (location 21, Table 1). The Point Rousse Complex contains fault-bounded blocks of serpentinized ultramafic rock including oceanic mantle (unit ЄMs) and layered ultramafic cumulate rocks (unit ЄBHu), and faulted blocks of layered gabbro and melagabbro (unit ЄBHg), massive gabbro, gabbro norite, and trondhjemite dated at 491 ± 5 Ma (location 23, Table 1). The upper section includes sheeted dykes (unit ЄBHs) and pillowed, light rare-earth element–depleted, island-arc tholeiitic basalt of the Mount Misery Formation. Boninitic lavas are not exposed; however, boninitic sheeted dykes are cut by plagioclase-phyric dykes of island-arc tholeiite affinity. The Advocate Complex includes kilometre-scale, fault-bounded tracts of serpentinized oceanic mantle and mantle harzburgite (unit ЄMh), and faulted blocks of layered ultramafic cumulate, layered melagabbro, pyroxenite and gabbro, and anorthositic gabbro and trondhjemite (unit ЄBHa). Massive gabbro (unit ЄBHm) is locally cut by dykes and altered to rodingite (unit ЄBHr) near serpentinized zones. Sheeted dykes (unit ЄBHs) include aphyric and plagioclase-phyric dykes. Boninite pillow breccia is rare and the majority of the pillow lavas belong to the Mount Misery Formation.

The Lower to Middle Ordovician Snooks Arm Group overlies the Baie Verte Oceanic Tract across Baie Verte Peninsula (Skulski et al., 2010). Basinward, the lower contact with the Pacquet and Point Rousse complexes is locally paraconformable and consists of a discontinuous magnetite–black chert iron-formation called the Nugget Pond member of the Scrape Point Formation (unit OSPi). Overlying the Advocate Complex, the basal Scrape Point Formation comprises megaconglomerate with decimetre-scale clasts of ophiolite-derived gabbro in a black shaly matrix (unit OSPx). The unexposed contact with the underlying Advocate Complex is interpreted to be an angular unconformity (Skulski et al., 2010). Overlying this unit is the Kidney Pond conglomerate (unit OSPc), a polymictic unit with clasts of ophiolite-derived gabbro, serpentinite, boninite, and of continental margin–derived marble, quartzite, and granitoid rock in a mixed sandy and shaly matrix. A sample of the granitoid clasts has a zircon age of 479 ± 4 Ma (location 18, *see* Skulski et al., 2015a, south of map area) representing a maximum age for sediment deposition. North of Flat Water Pond, the Mount Misery Formation is locally overlain by the Nugget Pond iron-formation. A felsic to intermediate volcanic unit (dacite-andesite) overlies this unit and has a zircon U/Pb age of 476.5 ± 4 Ma (location 17, Table 1; unit OSPf). The upper reaches of the Scrape Point Formation include pillowed, high TiO_2 (up to 3 weight per cent) tholeiitic basalt

(unit OSPm) and mafic volcaniclastic and epiclastic rocks (unit OSPv). Overlying these units is the Bobby Cove Formation, comprising plagioclase-phyric, calc-alkaline pillow basalt (unit OBCm), and a regionally distinct marker, the Prairie Hat member, consisting of clionopyroxene-phyric (locally replaced by amphibole) mafic crystal tuff, lapilli tuff, and tuff breccia dated at 470 ± 4 Ma (location 16, *see* Skulski et al., 2015b, east of the map area). The upper Bobby Cove formation includes mafic tuff (unit OBCv) and a westward-thinning mafic turbidite sequence of wacke, siltstone, and shale (unit OBCe) capped by a magnetite-chert iron-formation (unit OBCi). Renewed, tholeiitic mafic volcanism is marked by the appearance of the Venams Bight Formation (unit OVBm). The Balsam Bud Cove Formation overlies this unit and comprises volcaniclastic turbiditic wacke, black graphitic schist, and thin felsic tuff units (unit OBBs) that are dated over the Pacquet complex at 470 ± 4 Ma (location 15, *see* Skulski et al., 2015b, east of the map area). Tholeiitic pillow basalt units of the Round Harbour Formation mark the top of the stratigraphy (unit ORHm). Tholeiitic gabbro sills and dykes (unit OSAg) and diorite (unit OSad) cut both the underlying Pacquet complex and Snooks Arm Group. The Stog'er Tight gabbro sill near the base of the Scrape Point Formation has an imprecise zircon age of 483.1 +8.7/-4.8 Ma (location 20, Table 1). A 458 ± 4 Ma (location 13, Table 1) felsic, flow-banded dyke cuts the Snooks Arm Group overlying the southern Pacquet complex, and is coeval with deposition of the Black Brook formation south of the map area.

The Burlington plutonic suite marks a major transition in the Notre Dame Subzone to felsic plutonism and coeval subaerial volcanism in the Late Ordovician-Silurian (Llandovery-Wenlock) that was accompanied by episodic regional uplift and emergence of the continental margin sequence, and by the Wenlockian, was synchronous with the Salinic Orogeny (Skulski et al., 2010). The Burlington plutonic suite comprises an early phase of calc-alkaline, hornblende+biotite granodiorite (unit OBgdh) dated at 445 ± 4 Ma (location 11, Table 1), an intermediate, synvolcanic (*see* below) phase of biotite±hornblende granodiorite (unit SBgd) dated at 441 ± 1.2 Ma (location 9, Table 1), and a late ferroan phase of biotite granodiorite to monzogranite (unit SBgdb) dated at 433 ± 0.8 Ma (location 8, Table 1).

The Micmac Lake Group consists of two unconformity-bound, Silurian formations with redbeds and subaerial volcanic rocks: the Strugglers Pond, and overlying Fox Pond formations. The Strugglers Pond formation is best exposed south of the map area where it unconformably overlies the Burlington plutonic suite (unit OBgdh) and includes a basal red pebble to boulder conglomerate with clasts of granodiorite, rhyolite, quartz-feldspar porphyry, and basalt (unit SMSc). The conglomerate is overlain by massive basalt (unit SMSb). Felsic volcanic rocks in the Strugglers Pond formation south of the present map area have been dated at 442 ± 4 Ma (location 10, *see* Skulski et al., 2015a). The Fox Pond formation lies unconformably on the Strugglers Pond formation and Burlington plutonic suite, including the ca. 433 Ma monzogranite phase. The base contains massive basalt, basanite, and hawaiite (unit SMFb), overlain by alkaline basaltic to mugearitic lapilli tuff (unit SMFtb) dated at younger than 430 ± 4 Ma (location 7, Table 1), and volcanic- and plutonic-derived, pebble to boulder conglomerate
(unit SMFc). These are overlain by massive trachytic alkaline basalt (unit SMFt), arkosic sandstone (unit SMFs), and eutaxitic ignimbrite (unit SMFi).

The Confusion Bay plutonic suite and Cape St. John Group are exposed in the east and include the early synvolcanic Cape Brulé Porphyry consisting of melanocratic, porphyritic quartz-feldspar granodiorite to monzogranite (unit SMFb) and finer grained, locally modally layered, quartz-feldspar-biotite porphyritic monzogranite (unit SCBp; dated to the east at 429 ± 4 Ma; location 6, *see* Skulski et al., 2015b). The latter is cut by a quartz-feldspar porphyry (locally aplite) ring dyke (unit SCBd). The lower Cape St. John Group includes red arkose and pebbly sandstone of the Beaver Cove formation (unit SBCs; dated at 427.8 ± 0.6 Ma to the east; location 5, *see* Skulski et al., 2015b) and overlying, unseparated volcanic rocks (unit SCSJu). The Dunamagon Granite is a synvolcanic biotite monzogranite (unit SDgr) and is dated at 427.2 ± 1.4 Ma (location 4, *see* Skulski et al., 2015b). The King's Point volcanic complex is coeval with the Cape St. John Group and is exposed in the south. The Upper volcanic unit (unit SKqfa) consists of quartz-feldspar porphyritic comenditic ash-flow tuff, breccia, and possible hypabyssal intrusive equivalents, forming a prominent ring dyke. Feldspar±quartz porphyritic syenite form late synvolcanic stocks that are dated at 427 ± 2 Ma (Coyle, 1990). Post-tectonic intrusive rocks include massive leucocratic muscovite±garnet granite (unit SDPPg) that cuts tectonic fabrics on the northwestern shore of Baie Verte Peninsula.

ECONOMIC GEOLOGY

Ten mines have operated in the map area including two that are currently in production and eight that are past producing (Table 2; Hibbard, 1983; Evans, 2004). Numerous mineralized areas have also been explored by drilling (Table 3). The Terra Nova mine in the town of Baie Verte operated between 1860 and 1915. The deposit consists of lenses of copper-rich volcanogenic massive-sulphide ore that are hosted by the Mount Misery Formation. The Rambler mining camp includes the past-producing Rambler Main, Big Rambler Pond, and East mines, and the recently reopened, Ming and Ming West mines (Pilote and Piercey, 2013; Brueckner et al., 2014). These are copper-rich (±zinc), volcanogenic massive-sulphide orebodies with gold and silver mineralization. The Ming and Rambler deposits are massive and stratabound, and occur in the upper reaches of the Rambler Rhyolite formation. The East deposit is disseminated and stratabound and hosted in altered, distal felsic volcanic rocks. The Big Rambler Pond deposit has stockwork disseminated and stringer mineralization hosted in the Mount Misery Formation. The Advocate mine operated between 1963 and 1994 and produced asbestos hosted in serpentinized ultramafic rocks of the Advocate Complex. The Snooks Arm Group is host to three gold deposits on Point Rousse Peninsula. The Goldenville deposit (Hibbard, 1983; Evans, 2004) is a small past-producing gold deposit hosted by the Nugget Pond member of the Scrape Point Formation. Gold is associated with pyrite, quartz-pyrite, and quartz-carbonate-sulphide veins that cut beds of ferruginous chert, chlorite-magnetite, and massive magnetite iron-formation. A number of small gold deposits are associated with the iron-formation (Goldenville horizon of Evans, 2004) and these are correlated with the Nugget Pond member overlying the Betts Cove Complex (Skulski et al., 2010). The Stog'er Tight deposit is a small gold deposit hosted by locally altered, tholeiitic gabbro sills hosted in the Scrape Point Formation. Gold is associated with pyrite in albite-pyrite alteration cut by quartz-albite-ankerite veins (Ramezani, 1992; Ramezani et al., 2000; Evans, 2004). The Pine Cove deposit is an active gold mine on southern Point Rousse Peninsula (Evans, 2004;

Kerr and Selby, 2012). Gold mineralization is hosted by pervasively altered mafic volcanic rocks and gabbro and is associated with disseminated pyrite cut by discrete quartz veins and quartz-carbonate breccia (Kerr and Selby, 2012).

TECTONOMETAMORPHIC EVOLUTION

Notwithstanding the Grenvillian tectonometamorphism affecting the East Pond Metamorphic Suite (D_b of Hibbard (1983)), rocks of the western Baie Verte Peninsula have been affected by at least four phases of deformation (Castonguay et al., 2009 and Skulski et al., 2010 compiled from Gale, 1971; Kennedy, 1971; de Wit, 1972; Kidd, 1974; Bursnall, 1975; Tuach and Kennedy, 1978; Hibbard, 1983; Anderson, 1998; Anderson et al., 2001). Structural correlations across the Baie Verte Line are rendered difficult due to intense and long-lived strain along the complex fault zone, which has juxtaposed rock units of different origins and structural levels.

Structures and metamorphic imprint related to D_1 (D_e of Hibbard, 1983) are best preserved in the Birchy Complex, less so in the rest of the Fleur de Lys Supergroup, locally developed in the ophiolitic rocks, and absent in the cover sequence. Relict S_1 fabrics are preserved locally in the hinges of F_2 folds and are transposed on limbs of folds. Strongly overprinted D_1 fault zones are northwest-directed thrust faults that are commonly decorated with serpentinite in the Fleur de Lys Supergroup (Hibbard, 1983 and references therein). The D_1 phase is interpreted to be related to obduction of ophiolite complexes, partial underthrusting of the Humber margin and arc collision of the Baie Verte Oceanic Tract during the Taconic Orogeny (Waldron et al., 1998; van Staal et al., 2007). Age constraints on Taconic deformation and metamorphism vary from 467 Ma to 460 Ma in the Birchy Complex (location 51, 54, and 79, Table 1; $^{40}Ar/^{39}Ar$ amphibole and muscovite ages) and from 481 Ma to 465 Ma from the structural base of the Advocate Complex (location 73, 55, and 56, Table 1; $^{40}Ar/^{39}Ar$ amphibole ages). A concordant ca. 465 Ma U-Pb metamorphic zircon age (location 109, Table 1) was obtained from an amphibolitized eclogite in the East Pond Metamorphic Suite.

Penetrative D_2 deformation (D_m of Hibbard, 1983) and greenschist- to amphibolite-facies metamorphism affects all rock units of the Baie Verte Peninsula. Although locally folded, the S_2 foliation is generally steep, trending to the south-southwest in the Fleur de Lys Supergroup, Advocate Complex, and its cover rocks. D_2 is associated with tight folds and bivergent fault zones (southeast- and northwest-directed). In the Point Rousse and Pacquet complexes east of Baie Verte, the main S_2 foliation is southwest- to northwest-dipping, locally characterized by a strong L>S fabric, and is cogenetic with macroscopic F_2 folds and south-directed reverse faults and shear zones, such as the Scrape Thrust.

D_2 fabrics are locally overprinted by asymmetric and upright chevron F_3 folds, associated with an axial-planar S_3 strain-slip foliation (D_L of Hibbard, 1983). D_3 fabrics are apparently concentrated in zones (Kidd, 1974; Bursnall, 1975) and account for local deflection of the main structural grain. In the Birchy and Advocate complexes, D_3 (D_{2b} and D_3 of Kidd, 1974; D_3 of Bursnall, 1975) is associated with two sets of asymmetric folds. In the Pacquet complex, D_3 deformation (D_4 of Tuach and Kennedy, 1978) is characterized by undulating to close, northeast-trending and -plunging cross folds, locally associated with a subvertical fracture or crenulation cleavage. In the Point Rousse Complex and in the vicinity of the Scrape Thrust, D_3 folds and fabrics are related to sinistral east-directed transpressional shear zones (Kidd et al., 1978; Hibbard, 1983; Anderson, 1998). D_2 and D_3 are interpreted as part of an overall Salinic sinistral

transpressional regime (Waldron et al., 1998). The age of Salinic deformation and metamorphism is locally constrained to be between 432 Ma (location 57, Table 1; $^{40}Ar/^{39}Ar$ amphibole age) and 425 Ma (location 80, Table 1; $^{40}Ar/^{39}Ar$ muscovite age).

The fourth and fifth deformation phases (D_L of Hibbard (1983); D_2 and D_3 of Anderson et al. (2001)) are mainly documented along the Baie Verte Line, in and around the Ming's Bight Group, but also as reactivating (inverted) fault zones. A series of major, but relatively narrow steep fault zones (i.e. Baie Verte Road Fault and the Marble Cove Slide; Neale and Kennedy (1967); Hibbard (1983)) occur along the Baie Verte Line, and overprint earlier structural fabrics and shear zones. They are associated with small-scale, steeply plunging, dextral chevron F_4 folds and display dextral, compressional, or extensional kinematics (Goodwin and Williams, 1996; Anderson et al., 2001). Post D_2 (D_4 or D_5) extensional shear bands along the immediate footwall of the Scrape Thrust suggest that it was affected by normal-sense reactivation (Jamieson et al., 1993). In the Point Rousse Complex, extensional reactivation of D_2 faults is marked by moderately to steeply north-dipping crenulation, kink-bands, and shear bands suggesting brittle-ductile, north-side-down motion (Kidd et al., 1978; Anderson, 1998; Castonguay et al., 2009) compatible with the D_5 structures surrounding the Ming's Bight Group (D_3 of Anderson et al. (2001)). The composite $D_{4–5}$ phase is interpreted to have initiated during progressive Devonian extensional unroofing of the Ming's Bight Group and surrounding units, and was accompanied by amphibolite-facies metamorphism (405 Ma $^{40}Ar/^{39}Ar$ hornblende; location 65, Table 1 to 358 Ma $^{40}Ar/^{39}Ar$ muscovite; location 84, *see* Skulski et al., 2015b; both east of map area; Anderson et al. (2001)) during an overall dextral (transpressional to transtensional) regime (Waldron et al., 1998) across the Baie Verte Peninsula. Late transverse structures, such as the northwest-trending Advocate and Little Lobster Harbour faults (Bursnall, 1975; Hibbard, 1983) have apparent down-to-the-northeast normal offset, with a probable sinistral component and are cut by a late, north-trending dextral fault.

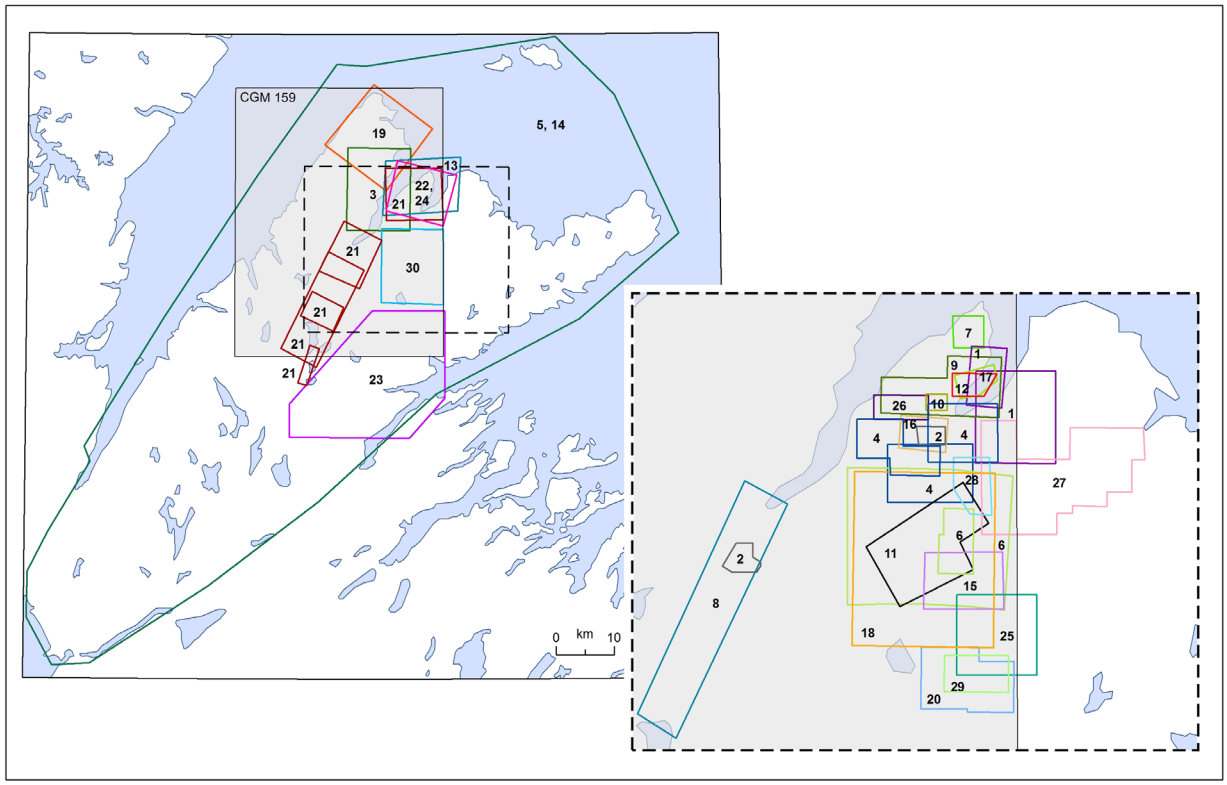

Figure 1. Map sources: 1 = Anderson, 1998; 2 = Bélanger, 1995; 3 = Bursnall, 1975; 4 = Christie and Dearin, 1986; 5 = Colman-Sadd and Crisby-Whittle, 2002; 6 = Dimmell and MacGillvray, 1991; 7 = Dubé et al., 1993; 8 = Dunsworth, 2004; 9 = Evans, 2004; 10 = Fitzpatrick, 1981; 11 = Gale, 1971; 12 = Gower, 1987a; 13 = Gower, 1987b; 14 = Hibbard, 1983; 15 = Huard, 1990a; 16 = Huard, 1990b; 17 = Jourdain and Oravec, 1996; 18 = Kambampati, 1984; 19 = Kennedy, 1971; 20 = Kerr and Collins, 1983; 21 = Kidd, 1974; 22 = Kidd et al., 1978; 23 = Miller and Abdel-Rahman, 1994; 24 = Norman, 1973; 25 = Piercey, 1996; 26 = Regular, 2005; 27 = Shepperd et al., 1987; 28 = Snow, 1989; 29 = Stewart, 1995; 30 = Tuach, 1976

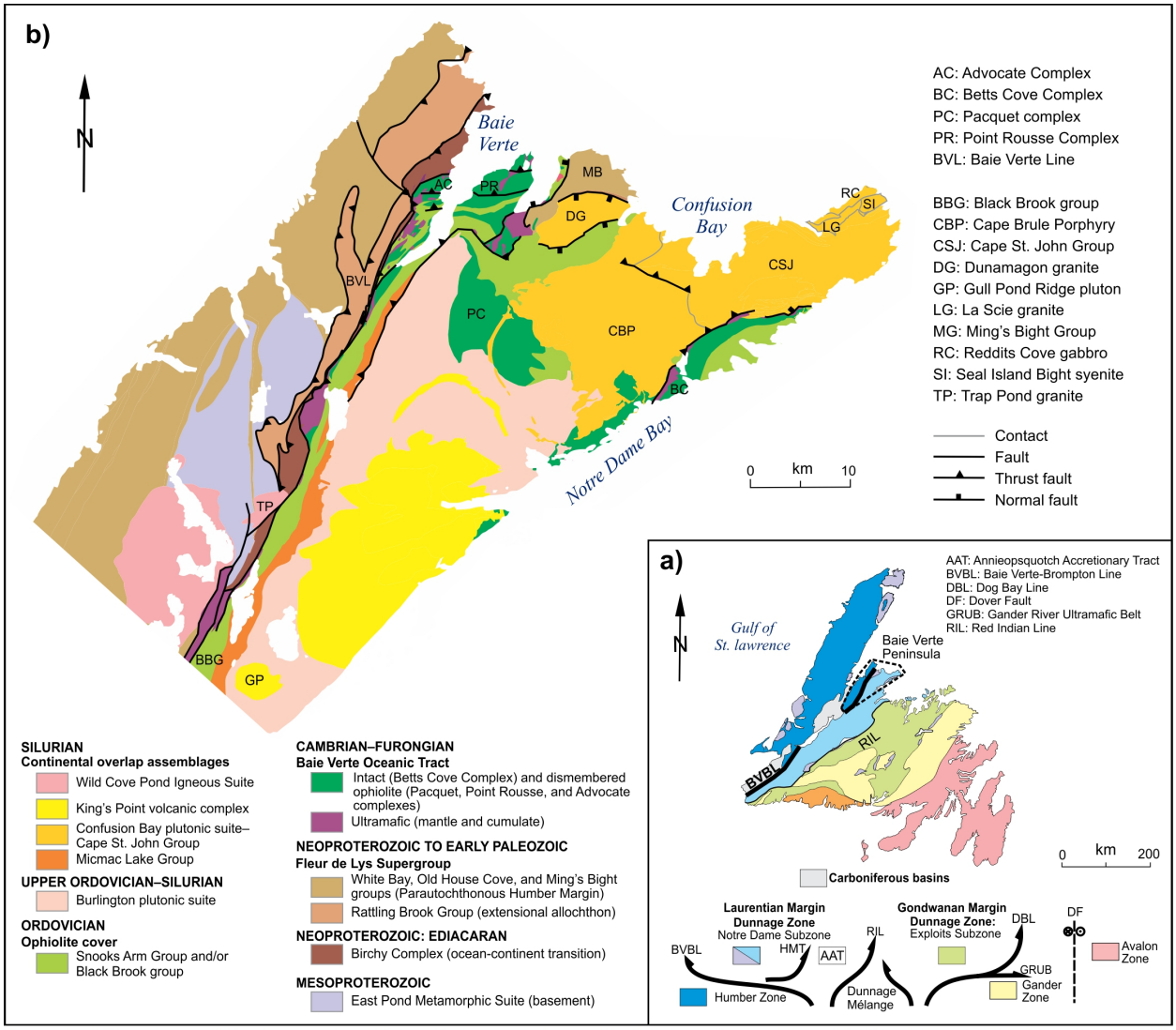

Figure 2. **a)** Tectonic map of Newfoundland and **b)** simplified geological map of the Baie Verte Peninsula (*modified from* Hibbard, 1983; Skulski et al., 2010; van Staal et al., 2013).

Location	Method	Mineral	Rock type	Code	Age (Ma)	Interpretation	Note	Reference
7	U/Pb SHRIMP	Zircon	Mafic lapilli tuff	SMFtb	<430 ± 4	Maximum crystallization age		Skulski et al., 2012
8	U/Pb-TIMS	Zircon, titanite	Biotite granite	SBgdb	433.0 ± 0.8	Weighted average of zircon		Skulski et al., 2012
9	U/Pb-TIMS	Zircon, titanite	Biotite±hornblende granodiorite	SBgd	441.0 ± 1.2	Weighted average of zircon		Skulski et al., 2012
11	U/Pb SHRIMP	Zircon	Hornblende-biotite Granodiorite	SBgdh	445 ± 4	Crystallization age		Skulski et al., 2012
13	U/Pb SHRIMP	Zircon	Quartz-feldspar porphyry dyke	uOqfp	458 ± 4	Crystallization age		Skulski et al., 2010
17	U/Pb SHRIMP	Zircon	Rhyolite flow	OSPf	476.5 ± 4	Crystallization age		Skulski et al., 2010
19	U/Pb-TIMS	Zircon	Amphibolite, metagabbro	CBHm	482.9 ± 0.8	Crystallization age		Skulski et al., 2010
20	U/Pb-TIMS	Zircon	Gabbro	OSAg	483.1 +8.7/-4.8	approximate age		Ramezani, 1992
21	U/Pb SHRIMP	Zircon	Rhyolite flow	CRRt	487 ± 4	Crystallization age		Skulski et al., 2010
23	U/Pb SHRIMP	Zircon	Tronchjemite	CBHs	491 ± 5	Crystallization age		*modified from* Skulski et al., 2010
24	U/Pb LA-ICPMS	Zircon	Intermediate tuffaceous schist	nPBg	556 ± 4	Crystallization age		van Staal et al., 2013
25	U/Pb-TIMS	Zircon	Metagabbro	nPBg	558.3 ± 0.7	Crystallization age		van Staal et al., 2013
26	U/Pb LA-ICPMS	Zircon	Hornblende metagabbro	nPBg	564 ± 7.5	Crystallization age		van Staal et al., 2013
27	U/Pb LA-ICPMS	Zircon	Muscovitic psammite	nPBFP	<990 ± 52	Maximum detrital age		van Staal et al., 2013
31	U/Pb-TIMS	Titanite	Hornblende biotite granodiorite	OBgdh	440.1 ± 0.7	Cooling age		Skulski et al., 2012
35	$^{40}Ar/^{39}Ar$ furnace step-heating	Amphibole	Mafic dyke	nPOa	393 ± 5	Metamorphic cooling age	Recalculated as 7 step plateau (100% ^{39}Ar); *see* note 2.	Dallmeyer, 1977
36	$^{40}Ar/^{39}Ar$ furnace step-heating	Amphibole	Mafic dyke	nPOOa	418 ± 5	Metamorphic cooling age	Recalculated as 5 step plateau (100% ^{39}Ar); *see* note 2.	Dallmeyer, 1977
37	$^{40}Ar/^{39}Ar$ furnace step-heating	Amphibole	Mafic dyke	nPOa	428 ± 5	Metamorphic cooling age	Recalculated as 5 step plateau (100% ^{39}Ar); *see* note 2.	Dallmeyer, 1977
38	$^{40}Ar/^{39}Ar$ furnace step-heating	Amphibole	Granodiorite	SBgdh	420 ± 10	Metamorphic cooling age	Plateau age, 89.2% gas release; *see* note 3.	Dallmeyer and Hibbard, 1984
39	$^{40}Ar/^{39}Ar$ furnace step-heating	Amphibole	Granodiorite	SBgd	409 ± 5	Metamorphic cooling age	*See* note 3.	Dallmeyer and Hibbard, 1984
42	$^{40}Ar/^{39}Ar$ furnace step-heating	Amphibole	Granodiorite	SBgd	416 ± 5	Metamorphic cooling age	*See* note 3.	Dallmeyer and Hibbard, 1984
43	$^{40}Ar/^{39}Ar$ furnace step-heating	Amphibole	Granodiorite	SBgd	417 ± 5	Metamorphic cooling age	*See* note 3.	Dallmeyer and Hibbard, 1984
45	$^{40}Ar/^{39}Ar$ furnace step-heating	Amphibole	Schist	OBCv	358 ± 5	Metamorphic cooling age	*See* note 3.	Dallmeyer and Hibbard, 1984
47	$^{40}Ar/^{39}Ar$ furnace step-heating	Amphibole	Granodiorite	SBgdh	467 ± 5	Inherited gas age	*See* note 3.	Dallmeyer and Hibbard, 1984
49	$^{40}Ar/^{39}Ar$ laser step-heating	Amphibole	Gabbro	OSAg	392.1 ± 10.3	Metamorphic cooling age	Plateau, 100% gas release.	Castonguay et al., 2010
50	$^{40}Ar/^{39}Ar$ laser step-heating	Amphibole	Mafic schist	nPBc	519.4 ± 3.4	Cooling age	Combined plateau from two aliquots, 88% gas released.	Castonguay et al., 2010
51	$^{40}Ar/^{39}Ar$ laser step-heating	Amphibole	Gabbro	nPBc	460.5 ± 14.2	Metamorphic cooling age	Plateau, 99% gas released.	Castonguay et al., 2014
52	$^{40}Ar/^{39}Ar$ laser step-heating	Amphibole	Gabbro	CBHs	453.5 ± 8.6	Metamorphic cooling age	Plateau,100% gas released.	Castonguay et al., 2014
54	$^{40}Ar/^{39}Ar$ laser step-heating	Amphibole	Mafic schist	nPBc	466.4 ± 6.5	Metamorphic cooling age	Pseudo-plateau, 86% gas released, 1 step dropped.	Castonguay et al., 2014
55	$^{40}Ar/^{39}Ar$ laser step-heating	Amphibole	Gabbro	CBHgc	465.1 ± 4.3	Metamorphic cooling age	Plateau,100% gas released.	Castonguay et al., 2014
56	$^{40}Ar/^{39}Ar$ laser step-heating	Amphibole	Gabbro	CBHm	470.2 ± 3.5	Metamorphic cooling age	Plateau, 79% gas released.	Castonguay et al., 2014
57	$^{40}Ar/^{39}Ar$ laser step-heating	Amphibole	Gabbro	CBHs	432.4 ± 3.2	Metamorphic cooling age	Plateau, 75% gas released.	Castonguay et al., 2010
58	$^{40}Ar/^{39}Ar$ laser step-heating	Amphibole	Basalt	CMMm	382.4 ± 4.2	Metamorphic cooling age	Combined plateau from two aliquots, 90% gas released.	Castonguay et al., 2010
67	$^{40}Ar/^{39}Ar$ furnace step-heating	Amphibole	Amphibolite	OVBm	388 ± 3	Metamorphic cooling age	Mylonitic amphibolite; *see* note 3.	Anderson et al., 2001
68	$^{40}Ar/^{39}Ar$ laser step-heating	Amphibole	Gabbro	CBHs	433.3 ± 4.3	Metamorphic cooling age	Inverse isochron age from 2 aliquots.	Castonguay et al., 2010
69	$^{40}Ar/^{39}Ar$ laser step-heating	Amphibole	Gabbro	CBHs	432 ± 3	Metamorphic cooling age	Combined plateau from three aliquots, 50% gas released.	Castonguay et al., 2010
70	$^{40}Ar/^{39}Ar$ laser step-heating	Amphibole	Gabbro	OSAg	383.4 ± 4.2	Metamorphic cooling age	Combined plateau from two aliquots, 100% gas released.	Castonguay et al., 2010
71	$^{40}Ar/^{39}Ar$ laser step-heating	Amphibole	Mafic schist	OBCm	380 ± 4.1	Metamorphic cooling age	Combined plateau from two aliquots, 100% gas released.	Castonguay et al., 2010
72	$^{40}Ar/^{39}Ar$ laser step-heating	Amphibole	Mafic schist	CMMm	347.3 ± 3.2	Metamorphic cooling age	Plateau, 60% gas released.	Castonguay et al., 2010
73	$^{40}Ar/^{39}Ar$ laser step-heating	Amphibole	Mafic schist	CBHm	481.2 ± 6.4	Metamorphic cooling age	Pseudo-plateau, 87% gas released, 2 steps dropped.	Castonguay et al., 2014
74	$^{40}Ar/^{39}Ar$ furnace step-heating	Muscovite	Schist	nPOOHp	398 ± 5	Metamorphic cooling age	Recalculated as six step plateau (100% ^{39}Ar); *see* note 2.	Dallmeyer, 1977
75	$^{40}Ar/^{39}Ar$ furnace step-heating	Muscovite	Schist	nPOOHp	424 ± 5	Metamorphic cooling age	Recalculated as five step plateau (95% ^{39}Ar); *see* note 2.	Dallmeyer, 1977
76	$^{40}Ar/^{39}Ar$ furnace step-heating	Muscovite	Schist	nPOOHp	419 ± 5	Metamorphic cooling age	Recalculated as six step plateau (100% ^{39}Ar); *see* note 2.	Dallmeyer, 1977
77	$^{40}Ar/^{39}Ar$ furnace step-heating	Muscovite	Schist	nPOOHp	401 ± 5	Metamorphic cooling age	Recalculated as six step plateau (100% ^{39}Ar); *see* note 2.	Dallmeyer, 1977
79	$^{40}Ar/^{39}Ar$ laser step-heating	Muscovite	Schist	nPBc	466.9 ± 2.5	Metamorphic cooling age	Plateau from two aliquots, 70% gas released, few steps dropped.	Castonguay et al., 2014
80	$^{40}Ar/^{39}Ar$ laser step-heating	Muscovite	Psammite	nPBc	424.9 ± 3	Recrystallization age	Plateau, 70% gas released.	Castonguay et al., 2014
90	$^{40}Ar/^{39}Ar$ furnace step-heating	Muscovite	Schist	nPOMB	370 ± 4	Metamorphic cooling age	Muscovite defines S_n; see note 4.	Anderson et al., 2001
92	$^{40}Ar/^{39}Ar$ laser step-heating	Muscovite	Carbonatized ultramafic rock	CBHu	408.4 ± 2.2	Metamorphic cooling age	Fuchsite, combined plateau from two aliquots, 70% gas released.	Castonguay et al., 2010
94	$^{40}Ar/^{39}Ar$ furnace step-heating	Biotite	Schist	nPOOHp	376 ± 5	Metamorphic cooling age	Total gas age from 6 steps; *see* note 2.	Dallmeyer, 1977
95	$^{40}Ar/^{39}Ar$ furnace step-heating	Biotite	Mafic dyke	nPOOHp	374 ± 5	Metamorphic cooling age	Total gas age from 7 steps; *see* note 2.	Dallmeyer, 1977
96	$^{40}Ar/^{39}Ar$ furnace step-heating	Biotite	Schist	nPOOHp	384 ± 5	Metamorphic cooling age	Total gas age from 6 steps; *see* note 2.	Dallmeyer, 1977
97	$^{40}Ar/^{39}Ar$ furnace step-heating	Biotite	Mafic dyke	nPOOHp	388 ± 5	Metamorphic cooling age	Total gas age from 6 steps; *see* note 2.	Dallmeyer, 1977
98	$^{40}Ar/^{39}A$ furnace step-heating	Biotite	Mafic dyke	nPOOHp	389 ± 5	Metamorphic cooling age	Total gas age from 6 steps; *see* note 2.	Dallmeyer, 1977
99	$^{40}Ar/^{39}Ar$ furnace step-heating	Biotite	Granodiorite	SBgdb	345 ± 5	Metamorphic cooling age	Plateau age 10 steps; see note 3.	Dallmeyer and Hibbard, 1984
100	$^{40}Ar/^{39}Ar$ furnace step-heating	Biotite	Granodiorite	SBgdb	347 ± 5	Metamorphic cooling age	Plateau age 10 steps; *see* note 3.	Dallmeyer and Hibbard, 1984
101	$^{40}Ar/^{39}Ar$ furnace step-heating	Biotite	Gneiss	mPEPm	394 ± 5	Metamorphic cooling age	Total gas age from 7 steps; *see* note 2.	Dallmeyer, 1977
102	$^{40}Ar/^{39}Ar$ furnace step-heating	Biotite	Granodiorite	SBgd	412 ± 10	Metamorphic cooling age	Discordant spectrum, total gas age; *see* note 3.	Dallmeyer and Hibbard, 1984
107	$^{40}Ar/^{39}Ar$ furnace step-heating	Biotite	Gabbro	OSAg	349 ± 5	Metamorphic cooling age	Four step plateau age; *see* note 3.	Dallmeyer and Hibbard, 1984
109	U/Pb SHRIMP	Zircon	Gabbro eclogite dyke	nPOae	465 ± 12	Metamorphic cooling age	Metamorphic zircon dates, amphibolitization of eclogite.	Castonguay et al., 2014
110	U/Pb SHRIMP	Zircon	Pink granite gneiss	mPEPm	1491 ± 19	Approximate age		de Wit and Armstrong, 2014
111	U/Pb SHRIMP	Zircon	Grey banded paragneiss	mPEPm	1073 ± 19	Detrital maximum age		de Wit and Armstrong, 2014

Notes

1 $^{40}Ar/^{39}Ar$ ages (new and historic data) have been calculated using a total ^{40}K decay constant of 5.463E-10 (Min et al., 2000). Some plateau ages (indicated in table) have been recalculated using Isoplot version 3.7 of Ken Ludwig using recalculated ages of steps (in light of revised decay constant and internal standard ages) using Noah Mclean's ArArReCalc_7-31-09.

2 Recalculated using age of Biotite standard SB-2 as 164 Ma revised from original value of 160.2 Ma in light of revised ^{40}K decay constant (note 1).

3 Recalculated using an age of MMhb-1 hornblende standard of 523.1 Ma (Renne et al., 1998) revised from original data calculated using an age of MMhb-1 of 519.5 Ma (Alexander et al., 1978).

4 Recalculated using an age of MMhb-1 hornblende standard of 523.1 Ma (Renne et al., 1998) revised from original data calculated using an age of MMhb-1 of 520 Ma (Samson and Alexander, 1987).

Table 1. Geochronological data.

Location	Name	Status	Commodity	Secondary commodity
4	Ming mine	Producing	Copper	Gold, silver, zinc
5	Ming West mine	Past producer	Copper	Gold, silver, zinc, lead
6	East mine	Past producer	Copper	Gold, silver
7	Rambler Main mine	Past producer	Copper	Gold, silver, zinc, cadmium, lead
8	Deer Cove mine	Past producer	Gold	Gold
9	Big Rambler Pond mine	Past producer	Copper	Gold
10	Goldenville mine	Past producer	Gold	Copper, iron
11	Stog'er Tight mine	Past producer	Gold	Silver, copper, molybdenum, zinc
12	Pine Cove mine	Producing	Gold	
13	Terra Nova mine	Past producer	Copper	Gold, silver
14	Baie Verte mine	Past producer	Asbestos	

Table 2. Past and current mines.

Location	Name	Commodity	Secondary commodity
1	Mud Pond	Copper	
2	Anoroc/Anoroc Extension	Gold	
3	Romeo and Juliet	Gold	
8	Deer Cove (#6)	Gold	
10	West Pond	Asbestos	
12	Priest's Prospect	Copper	Gold
14	L5 Target	Copper	
16	Dorset	Gold	
19	1807 Zone	Copper	Gold
20	Hodder	Copper	Marble
21	Dorset Extension	Gold	
22	Carb/Fuel Bog	Gold	
23	Balcony	Gold	
26	Pine Cove-Western Extension	Gold	
29	Fox Pond #2	Gold	Copper, talc
30	CRML 6851-1	Copper	Gold
31	Biarritz	Gold	
32	Corner Shore	Gold	
33	Brass Buckle	Gold	
34	Krissy Trend	Gold	Silver, copper
37	Cabot Graphite	Graphite	
38	Cabot	Copper	Cobalt, zinc
39	Upper Ming Footwall	Copper	Gold
43	South Brook Gold	Gold	Silver, copper, zinc
45	Parrell	Molybdenum	Copper, lead
46	Traverstown	Lead	

Table 3. Drilled prospects.

References

Alexander, E.C., Jr., Mickelson, G.M., and Lanphere, M.A., 1978. MMhb-1; a new ^{40}Ar-^{39}Ar dating standard; in International Conference on Geochronology, Cosmochronology, and Isotope Geology, 4th, Snowmass-at-Aspen, Colorado, 1978, Short Papers; U.S. Geological Survey, Open-File Report 78-701, p. 6–8.

Anderson, S.D., 1998. Structure, metamorphism, and U–Pb and $^{40}Ar/^{39}Ar$ geochronology of the Ming's Bight Group, and the Paleozoic tectonic evolution of the Baie Verte Peninsula, Newfoundland; Ph.D. thesis, Dalhousie University, Dartmouth, Nova Scotia, 452 p.

Anderson, S.D., Jamieson, R.A., and Reynolds, P.H., 2001. Devonian extension in northwestern Newfoundland: $^{40}Ar/^{39}Ar$ and U-Pb data from the Ming's Bight area, Baie Verte Peninsula; Journal of Geology, v. 10, p. 191–211.

Bélanger, M., 1995. Contrôle structurale et contexte métallogenique de l'indice aurifère Dorset, Péninsule de Baie Verte, Terre-Neuve; M.Sc. thesis, INRS-Géoressources, Québec, Quebec, 81 p.

Brueckner, S.M., Piercey, S.J., Sylvester, P.J., Maloney, S., and Pilgrim, L., 2014. Evidence for syngenetic precious metal enrichment in an Appalachian volcanogenic massive sulfide system: the 1806 zone, Ming mine, Newfoundland, Canada; Economic Geology, v. 109, p. 1611–1642.

Bursnall, J.T., 1975. Stratigraphy, structure and metamorphism west of Baie Verte, Burlington Peninsula, Newfoundland; Ph.D. thesis, Cambridge University, Cambridge, United Kingdom, 337 p., scale 1:12 500.

Castonguay, S., Skulski, T., van Staal, C., and Currie, M., 2009. New insights on the structural geology of the Pacquet Harbour Group and Point Rousse Complex, Baie Verte Peninsula, Newfoundland; Newfoundland and Labrador Department of Natural Resources, Geological Survey, Current Research 2009, Report 09-1, p. 147–158.

Castonguay, S., Skulski, T., van Staal, C.R., McNicoll, V., Joyce, N., 2010. Revisiting the Baie Verte Flexure: from Silurian transpression to Devonian transtension, a long-lived oblique transfer zone, Baie Verte Peninsula, Newfoundland Appalachians; *in* Abstracts with Programs, Geological Society of America, Northeastern and Southeastern Sections Joint Annual Meeting, March 13–16, Baltimore, Maryland, p. 164.

Castonguay, S., van Staal, C.R., Joyce, N., Skulski, T., and Hibbard, J., 2014. Taconic metamorphism preserved in the Baie Verte Peninsula, Newfoundland Appalachians:

geochronological evidence for ophiolite obduction and subduction and exhumation of the leading edge of the Laurentian (Humber) margin during closure of the Taconic Seaway; Geoscience Canada, v. 41, p. 459–482.

Christie, B.J. and Dearin, C., 1986. Geological report on phase 1 and recommended phase 2 exploration programs for the Ming's Bight claim group, Baie Verte Peninsula, Newfoundland; Newfoundland Department of Energy and Mines Assessment Report 012H/16/0965, 18 p.

Cohen, K.M., Finney, S.M., Gibbard, P.L., and Fan, J.-X., 2013. The ICS International Chronostratigraphic Chart; Episodes, v. 36, p. 199–204.

Colman-Sadd, S.P. and Crisby-Whittle, L.V.J., 2002. Partial bedrock geology dataset of the Island of Newfoundland (NTS areas 02 E, 12 H, 12 G, and parts of 01 M, 02 D, 02 L, 12 A, 12 B, and 12I); Newfoundland and Labrador Department of Mines and Energy, Open File NFLD/2616.

Coyle, M., 1990. Geology, geochemistry and geochronology of the Springdale Group, an Early Silurian caldera in central Newfoundland; Ph.D. thesis, Memorial University of Newfoundland, St. John's, Newfoundland and Labrador, 310 p.

Dallmeyer, R.D., 1977. $^{40}Ar/^{39}Ar$ age spectra of minerals from the Fleur de Lys terrane in northwest Newfoundland: their bearing on chronology of metamorphism within the Appalachian orthotectonic zone; Journal of Geology, v. 85, p. 89–103.

Dallmeyer, R.D. and Hibbard, J., 1984. Geochronology of the Baie Verte Peninsula, Newfoundland: implications for the tectonic evolution of the Humber and Dunnage Zones of the Appalachian Orogen; Journal of Geology, v. 92, p. 489–512.

de Wit, M.J., 1972. The geology around Bear Cove, eastern White Bay, Newfoundland; Ph.D. thesis, University of Cambridge, Cambridge, England, 232 p.

de Wit, M.J., 1980. Structural and metamorphic relationships of pre-Fleur de Lys and Fleur de Lys rocks of the Baie Verte Peninsula, Newfoundland; Canadian Journal of Earth Sciences, v. 17, p. 1559–1575.

de Wit, M.J. and Armstrong, R., 2014. Ode to field geology of Williams: Fleur de Lys nectar still fermenting on Belle Isle; Geoscience Canada, v. 41, p. 118–137.

Dimmell, P.M. and MacGillivray, G., 1991. 1990 Assessment report on the project 7451-Wellsdale option, Baie Verte, Newfoundland, M.L. 127 (12053) fee simples – vol 1, fol 82 & 83; Newfoundland Department of Energy and Mines, Assessment Report 12H/16-1220, 124 p.

Dubé, B., Lauzière, K., and Poulsen, H.K., 1993. The Deer Cove deposit: an example of "thrust" related breccia-vein type gold mineralization in the Baie Verte Peninsula, Newfoundland; *in* Current Research, Part D; Geological Survey of Canada, Paper 93-1D, p. 1–10.

Dunsworth, S., 2004. Assessment report of prospecting, geochemical mapping, sampling and geochemistry on licenses #9005M (year 2 supplementary), #9068M (year 2), #7825M (year 4), #7300M (year 5), #7486M (year 5) and 7299M (year 5), The Dorset Property, NTS 12H/16, Baie Verte Newfoundland; Newfoundland Department of Energy and Mines, Assessment Report 012h/16/1738, 45 p.

Evans, D.T.W., 2004. Epigenetic gold occurrences, Baie Verte Peninsula (NTS 12H/09, 16 and 12I/01), Newfoundland; Government of Newfoundland and Labrador, Department of Natural Resources, Geological Survey, Mineral Resources Report no. 11, 157 p.

Fitzpatrick, D.S., 1981. Geology and mineral potential of upper ophiolitic rocks near Ming's Bight, Burlington Peninsula, Newfoundland; B.Sc. thesis, Memorial University of Newfoundland, St. John's, Newfoundland and Labrador, 90 p.

Gale, G.H., 1971. An investigation of some sulphide deposits in the Rambler area, Newfoundland; Ph.D. thesis, University of Durham, Durham, England, 137 p.

Goodwin, L.B. and Williams, P.F., 1996. Deformation path partioning within a transpressive shear zone, Marble Cove, Newfoundland; Journal of Structural Geology, v.18, p. 975–990.

Gower, D., 1987a. Maritec Option, NTS 12H/16 License #2471, C.B. 3668 Report on Geochemical surveys and prospecting; Newfoundland Mineral, Lands and Mines Division, Assessment Report 12H/16/987, 127 p.

Gower, D., 1987b. Third year assessment report on diamond drilling, geological mapping, trenching, underground exploration, geophysical and geochemical surveys licences 2463 and 2878 Devil's Cove claim group, NTS 12I/1, 12H/16; Newfoundland Mineral, Lands and Mines Division, Assessment Report NFLD 1744, 35 p.

Hibbard, J., 1983. Geology of the Baie Verte Peninsula, Newfoundland; Department of Mines and Energy, Government of Newfoundland and Labrador, Memoir 2, 279 p., scale 1:100 000.

Huard, A., 1990a. Fourth year assessment report geological and geochemical licence 2745 Shear South property, NTS 12H/16; Newfoundland Department of Energy and Mines, Assessment Report 12H/16-1152, 43 p.

Huard, A., 1990b. Fifth Year Assessment Report, Licence 4078 Trenching and diamond drilling Bradley north property NTS 12H/16; Newfoundland Mineral, Lands and Mines Division, Assessment Report 12H/16/1229, 4 p.

Jamieson, R.A., Anderson, S.D., and McDonald, L., 1993. Slip on the Scrape – an extensional allochthon east of the Baie Verte Line Newfoundland; *in* Geological Society of America, Abstracts with Programs, v. 25, no. 2, p. 26.

Jourdain, V. and Oravec, K., 1996. Geological compilation and assessment of exploration 1996, Goldenville-east property, Baie Verte Peninsula, Newfoundland; Newfoundland Mineral, Lands and Mines Division, Assessment Report 12H/16/1436, 45 p.

Kambampati, M.V., 1984. Geology, petrochemistry and tectonic setting of the Rambler area, Baie Verte Peninsula, Newfoundland; M.Sc. thesis, University of New Brunswick, Fredericton, New Brunswick, 268 p.

Kennedy, M.J., 1971. Structure and stratigraphy of the Fleur de Lys Supergroup in the Fleur de Lys area, Burlington Peninsula, Newfoundland; *in* Proceedings of the Geological Association of Canada, v. 24, p. 59–73.

Kerr, A. and Collins, M.J., 1983. Iron Ore Company of Canada Gull Pond Project, report on geology, geophysics, geochemistry and diamond drilling, Licence 2220, 2224, NTS 12 H/16, Baie Verte Area, Newfoundland; Newfoundland Department of Energy and Mines, Assessment Report 12H/16-811/1-11, 63 p.

Kerr, A. and Selby, D., 2012. The timing of epigenetic gold mineralization on the Baie Verte Peninsula, Newfoundland, Canada: new evidence from Re-Os pyrite geochronology; Mineralum Deposita, v. 47, p. 325–337.

Kidd, W.S.F., 1974. The evolution of the Baie Verte lineament, Burlington Peninsula, Newfoundland; Ph.D. thesis, University of Cambridge, Cambridge, England, 294 p.

Kidd, W.S.F., Dewey, J.F., and Bird, J.M., 1978. The Mings Bight ophiolite complex, Newfoundland; Appalachian oceanic crust and mantle; Canadian Journal of Earth Sciences, v. 15, no. 5, p. 781–804.

Miller, R.R. and Abdel-Rahman, A.M., 1994. Geology of the King's Point Complex (parts of NTS 12H/9 and 12H/16), Newfoundland; Department of Mines and Energy, Newfoundland and Labrador, Map 2003-23, scale 1:50 000.

Min, K., Mundil, R., Renne, P.R., and Ludwig, K.R., 2000. A test for systematic errors in $^{40}Ar/^{39}Ar$ geochronology through comparison with U/Pb analysis of a 1.1 Ga rhyolite; Geochimica et Cosmochimica Acta, v. 64, p. 73–98.

Neale, E.R.W. and Kennedy, M.J., 1967. Relationship of the Fleur de Lys Group to younger groups of the Burlington Peninsula, Newfoundland; *in* Geology of the Atlantic Region, Hugh Lilly Memorial Volume, (ed.) E.R.W. Neale,and H. Williams; Geological Association of Canada, Special Paper 4, p. 139–169.

Norman, R.E., 1973. Geology and petrochemistry of ophiolitic rocks of the Baie verte Group exposed at Ming's Bight, Newfoundland; M.Sc. thesis, Memorial University of Newfoundland, St. John's, Newfoundland and Labrador, 122 p.

Piercey, J.P., 1996. The geology and geochemistry of the Southern Pacquet Harbour Group volcanics, Baie Verte Peninsula, Newfoundland; B.Sc. thesis, Memorial University of Newfoundland, St. John's, Newfoundland and Labrador, 123 p.

Pilote, J.-L. and Piercey, S.J., 2013. Volcanostratigraphy of the 1807 zone of the Ming Cu-Au volcanogenic massive-sulphide deposit, Baie Verte Peninsula, northern Newfoundland; Geological Survey of Canada, Current Research 2013-20, 13 p. doi:10.4095/293128

Ramezani, J., 1992. The geology, geochemistry and U/Pb geochronology of the Stog'er Tight Gold prospect Baie Verte Peninsula, Newfoundland; M.Sc. thesis, Memorial University of Newfoundland, St. John's, Newfoundland and Labrador, 256 p.

Ramezani, J., Dunning, G.R., and Wilson, M.R., 2000. Geologic setting, geochemistry of alteration, and U/Pb age of hydrothermal zircon from the Silurian Strog'er Tight gold prospect, Newfoundland Appalachians, Canada; Exploration and Mining Geology, v. 9, p. 171–188.

Regular, K., 2005. Seaside Realty Limited, eleventh year assessment report on the Big Bear property, Ming's Bight area, NL, License number 10238M, N.T.S. 12 H/16; Newfoundland Department of Energy and Mines, Assessment Report 12H/16-1748/1-2, 53 p.

Renne, P.R., Swisher, C.C., Deino, A.L., Karner, D.B., Owens, T.L., and Depaolo, D.J., 1998. Intercalibration of standards, absolute ages and uncertainties in $^{40}Ar/^{39}Ar$ dating; Chemical Geology, v. 145, p. 117–152.

Samson, S.D. and Alexander, E.C., 1987. Calibration of the interlaboratory $^{40}Ar/^{39}Ar$ dating standard, MMhb-1; Chemical Geology, Isotope Geoscience Section, v. 66, p. 27–34.

Sheppard, B., Strickland, R., Mercer, B., and Delaney, P., 1987. Exploration Report on Baie Verte Property licence# 3041, CB-5015-5017, 5020-5023, License 3154, CB 5330; Newfoundland Mineral, Lands and Mines Division, Assessment Report Nfld1866, 183 p.

Skulski, T., Castonguay, S., McNicoll, V., van Staal, C.R., Kidd, W., Rogers, N., Morris, W., Ugalde, H., Slavinski, H., Spicer, W., Mousallam, Y., and Kerr, I., 2010. Tectonostratigraphy of the Baie Verte Oceanic Tract and its ophiolite cover sequence on the Baie Verte Peninsula, Newfoundland; Newfoundland and Labrador Department of Natural Resources, Geological Survey, Current Research 2010, Report 10-1, p. 315–335.

Skulski, T., McNicoll, V., Whalen, J.B., Moussallam, Y., Dunning, G., Castonguay, S., Cawood, P., Kidd, W.S.F., and van Staal, C., 2012. Subduction to slab-break-off transition recorded in the timing, composition and setting of early Silurian volcano-plutonic complexes, Baie Verte Peninsula, Newfoundland; Geological Association of Canada–Mineralogical Association of Canada, Program with Abstracts, St. John's, Newfoundland, May 27–29, 2012, v. 35, p. 128.

Skulski, T., Castonguay, S., Kidd, W.S.F., McNicoll, V.J., and van Staal, C.R., 2015a. Geology, King's Point, Newfoundland and Labrador, NTS 12-H/9; Geological Survey of Canada, Canadian Geoscience Map 156, scale 1:50 000. doi:10.4095/295864

Skulski, T., Castonguay, S., Moussallam, Y., McNicoll, V.J., van Staal, C.R., and Bédard, J.H., 2015b. Geology, Nippers Harbour and parts of Horse Islands, Cape St. John, and Little Bay Island, Newfoundland and Labrador, NTS 2-E/13 and parts of NTS 2-E/12, NTS 2-E/14, NTS 2-L/4; Geological Survey of Canada, Canadian Geoscience Map 160, scale 1:50 000. doi:10.4095/295866

Snow, P., 1989. Third year assessment report on Shear rambler North property, Golden Havilah option, Licence 2744, NTS 12 H16 Newfoundland Department of Energy and Mines, Assessment Report 12H/16-1082, 140 p.

Stewart, P.W., 1995. Report on 1994 Exploration Gull Pond Property, Baie Verte Peninsula, Newfoundland, NTS 12 H/16, project 223; Newfoundland Department of Energy and Mines, Assessment Report 12H/16-1443, 31 p.

Tuach, J., 1976. Structural and stratigraphic setting of the Ming and other sulphide deposits in the Rambler area, Newfoundland; M.Sc. thesis, Memorial University of Newfoundland, St. John's, Newfoundland and Labrador, 123 p.

Tuach, J. and Kennedy, M.J., 1978. The geologic setting of the Ming and other sulfide deposits, Consolidated Rambler Mines, northeast Newfoundland; Economic Geology, v. 73, p. 192–206.

van Staal, C.R., Chew, D.M., Zagorevski, A., McNicoll, V., Hibbard, J., Skulski, T., Castonguay, S., Escayola, M.P., and Sylvester, P.J., 2013. Evidence of Late Ediacaran hyperextension of the Laurentian Iapetan margin in the Birchy Complex, Baie Verte Peninsula, northwest Newfoundland: implications for the opening of Iapetus, formation of peri-Laurentian microcontinents and Taconic–Grampian orogenesis; Geoscience Canada, v. 40, p. 94–117.

van Staal, C.R., Whalen, J.B., McNicoll, V.J., Pehrsson, S., Lissenberg, C.J., Zagorevski, A., van Breemen, O., and Jenner, G.A., 2007. The Notre Dame arc and the Taconic orogeny in Newfoundland; *in* 4-D Framework of Continental Crust, (ed.) R.D. Hatcher, Jr., M.P. Carlson, J.H. McBride, and J.R. Martínez Catalán; Geological Society of America, Memoir 200, p. 511–552.

Waldron, J.W.F., Anderson, S.D., Cawood, P.A., Goodwin, L.B., Hall, J., Jamieson, R.A., Palmer, S.E., Stockmal, G.S., and Williams, P.F., 1998. Evolution of the Appalachian Laurentian margin: Lithoprobe results in western Newfoundland; Canadian Journal of Earth Sciences, v. 11, p. 1271–1287.

Author Contact

Questions, suggestions, and comments regarding the geological information contained in the data sets should be addressed to:

Tom Skulski
Geological Survey of Canada
601 Booth Street
Ottawa, Ontario
K1A 0E8
Tom.Skulski@canada.ca

Coordinate System

Projection: Universal Transverse Mercator
Units: metres
Zone: 21
Horizontal Datum: NAD83
Vertical Datum: mean sea level

Bounding Coordinates

Western longitude: 56°30’00”W
Eastern longitude: 56°00’00”W
Northern latitude: 50°10’00”N
Southern latitude: 49°45’00”N

Data Model Information

This Canadian Geoscience Map does not conform to either the Bedrock or Surficial Mapping Geodatabase Data Models. The author may have included a complete description of the feature classes and attributes in the Data\Data Model Info folder.

LICENCE AGREEMENT

ACCORD DE LICENCE